NEW ZEALAND SOCIETY FOR EARTHQUAKE ENGINEERING
2019 Pacific Conference on Earthquake Engineering
TURNING HAZARD AWARENESS INTO RISK MITIGATION
4 – 6 April | SkyCity, Auckland | New Zealand

Numerical and experimental study on friction connections performance-asymmetric and symmetric (AFC/SFC)

M. Hatami, G. MacRae & G. Rodgers
University of Canterbury, Christchurch, New Zealand

C. Clifton
University of Auckland, Auckland, New Zealand.

ABSTRACT

This paper presents experimental test results and a finite element model validation of Asymmetric Friction Connections (AFC) and Symmetric Friction Connections (SFC) under a quasi-static cyclic sliding displacement regime. The experimental tests were conducted using M24 bolts. The numerical simulation of friction connections was developed using the finite element software ABAQUS. It was shown that the AFC and SFC hysteresis shapes are almost rectangular with the significant differences in the magnitude of strength, bolt force reduction during the sliding, damage severity and wear mechanism and reparability. Calibrated finite element model results were in good agreement with the experimental results under cyclic quasi-static loading regime. The numerical stress distribution, equivalent plastic strain, and the bolt force obtained at different sliding displacements were validated with the experimental tests. Effective friction coefficient varied between 0.14 to 0.18 for the AFC with wire brushed surfaces and 0.40 to 0.48 for the SFC with a similar configuration and preparation. The maximum strength reached 410 kN and 125 kN during the second run for the SFC and the AFC respectively. The wear mechanism and damage severity regarding volume and geometry of loose wear particles and formed grooves are higher in the SFC due to the higher friction coefficient as a result of different frictional behaviour in sliding surfaces. The loss of pretension force for the AFC reached 45% after 5250 mm cumulative travel, and it was 9.0% for the SFC. The maximum strength degradation reached 15% and 20% for the SFC and the AFC respectively. Both AFC and SFC are reparable connections. After replacing bolts and/or shims both configurations gave almost stable hysteresis behaviour to 13125 mm cumulative travel.

1 INTRODUCTION

Pall and Marsh (1982) introduced sliding friction devices and used them in the steel frame the bracing system. Asbestos brake lining pads were adapted to be shims to increase the friction between the plates and improve sliding shear capacity in connection. Pall and Marsh observed that the energy was dissipated on the friction surfaces and there was no localized plasticity in the main members. The hysteresis loops were rectangular and stable. Slotted Bolted Connections were introduced and tested by FitzGerald et al. (1989). Then Symmetric Friction Connections were developed (SFC) by Grigorian and Popov (1994) based on SBC, and they obtained a stable friction force using a brass shim material in contact with mild. Tremblay (1993) tested a large number of SFC as a component test and also in concentrically braced frames with various shim materials. It was suggested dissimilar materials should be used on sliding surfaces to reach more stable hysteresis behaviour. Further experimental tests on SFC were conducted by Yang and Popov (1995). Asymmetric Friction Connections (AFC) were applied at Sliding Hinge Joints as a low damage beam-column connection by Clifton (2005) and then further developed by MacRae et al. (2010).

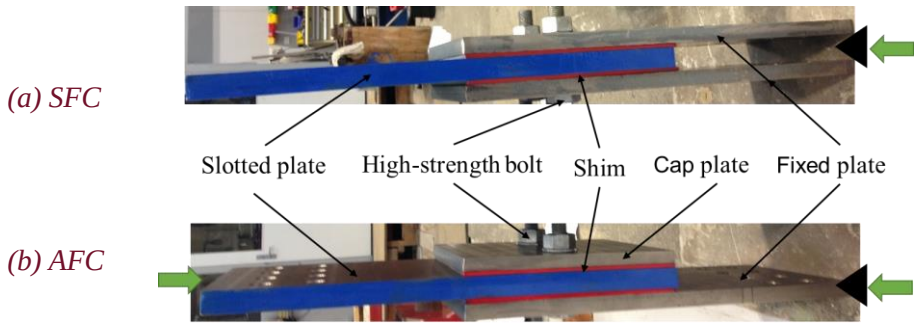

Figure 1: AFC and SFC components

Figures 1a and 1b show that SFC and AFC component respectively for some recent tests. Comprise a Grade 300 sliding plate with slotted holes, a Grade 300 steel fixed plate with normal holes, and two steel shims of harder material (here Bisalloy Grade 500). The AFC has another Grade 300 steel plate which is not connected to any support and acts as a large washer referred to the cap plate. For the SFC there is a second fixed plate, and the slotted plate slides between the two fixed plates symmetrically. All these plates are held together using high strength structural bolts Grade 8.8 or 10.9 which usually are tightened to their proof load. Structural; or Belleville washers may also be used. Recently A large number of experimental tests were conducted by Chanchi et al. (2012), Golondrino et al. (2016). He investigated different effective factors on the behaviour of AFC with 2 M16 bolts. Bisalloy 500 shim material has been recommended to have more reliable and predictable strength compared to other shim materials. Although there are a large number of studies on friction connections and their application on the buildings, there is a need to quantify differences between SFC and AFC with same configuration and same testing condition using bolts of a realistic size, which are pushed to large sliding displacements. This paper seeks to answer the following questions:

What is the physical performance of AFC compared to SFC?

How does the hysteretic performance change with AFC and SFC?

How do the bolt force and friction coefficient differ for AFC and SFC?

What are the design implications of the findings above?

2 EXPERIMENTAL TEST

Experimental tests were conducted on one AFC specimen and one SFC specimen with Bisalloy Grade 500 as shim material. Here the results of 10 runs on two specimens are discussed. In this paper AFC and SFC tests are shown by the notation A# and S# respectively. Where the number after # is the number of each run. In both cases, after the first run, enough time was allocated to the specimens to cool down and then the second run was conducted without any changes in the bolt tension force, surface condition or loading regime. At the end of this run, the two bolts were replaced by the new bolts, tightened to the same force, and the third run was started. Then after the tested bolts were removed as well as two steel shims and the slotted plate surfaces.

The fixed plate and cap plate surfaces were cleaned entirely from all hard particles, dust and debris. The new shims with the same hardness and similar roughness were placed on the specimens and clamped by two new bolts which were the fourth run. The last fifth run was conducted identically to the second run as a repeated test of prior run. Before assembly, all the surfaces were cleaned by acetone from any greases and dust. Also all sliding surfaces fully wire brushed, and all rusts and sharp edges due to cutting and drilling were removed. The cleaning step also was applied for all the structural bolts before tightening which include cleaning as received bolts from any external particle and lubricant and then applying Opal Hi-Load as a high-quality multipurpose grease containing molybdenum disulphide in all threaded parts 'MOLYBOND' (2019)

SFC comprised the steel plates Grade 300, Bisalloy Grade 500 ('Bisalloy Steels,Bisplate.technical guide' (2015)) with Brinell hardness values of 480 HB and two M24×160 mm long (95 mm shank and 32 mm threads as grip length) high-strength structural bolts Grade 8.8 and two structural washers to AS/NZS 1252 (2016) which were tightened to provide 210 kN tension force as their required proof load level NZS 3404 (2009).The slotted plate was 600×250×32 mm with two 200 mm long and 26 mm wide slotted holes. All other plate holes were 2 mm oversize for the M24 bolts (26 mm). The two fixed plates were 600×250×25 mm, and the shims were 300×250×6 mm. The AFC specimen was assembled with the same plates as per the SFC test except for the cap plate which was 300×250×20 mm.

Specimens were tested using the Dartec 10 MN universal testing machine using two slip-critical connections are used to connect the specimen to the top and bottom (moving) brackets of the Dartec. The brackets were designed using 40 mm width steel plate vertical stiffeners welded to a 60 mm circular plate. For the AFC 34 mm eccentricity between the centre of the top and the bottom vertical plates to alien the AFC as much as possible. Shims plate were provided for SFC tests to avoiding eccentricity. Although the Dartec has an internal load cell (for the maximum capacity), another 1000 kN load cell was calibrated. This was attached to the frame from the top. Then the fixed bracket was connected to the load cell with 10 M26 Dartec bolts, and the bottom bracket was bolted to the hydraulic ram by 6 M50 Dartec bolts. These bolts were hand tightened. The specimen was attached to the vertical plate of the fixed bracket at the top as well as the moving bracket at the bottom using eight M24 high-strength proof loaded bolts.

A linear and a rotational potentiometer, surface roughness meter model SJ-210 'Mitutoyo' (2019), two 400 kN force washers model 'HBM' (2019) and two 300 kN force washers model 'LCM SYSTEMS') were used for test instrumentation. Torque Gun-S2000 'HYTORC' (2019) was used for the bolt tightening. The bolt force after tightening and within the sliding tests was measured by the force washers and an ultrasonic tension monitor 'DAKOTA' (2019). Two potentiometers were located between the fixed plate and the fixed bracket. Also, two were placed between the slotted plate and the moving bracket to measure relative slip, which was expected to be zero. The AFC the cap plate-fixed plate and the slotted plate-fixed plate relative displacements were captured by a linear and rotational potentiometer. Two force washers (load cells) were located between the bolt's head and the fixed plates to record the clamping force after the bolt's tightening and throughout the sliding tests. The bolt head and the nut rotation (turn angle) were measured after the tightening and at the end of each test.

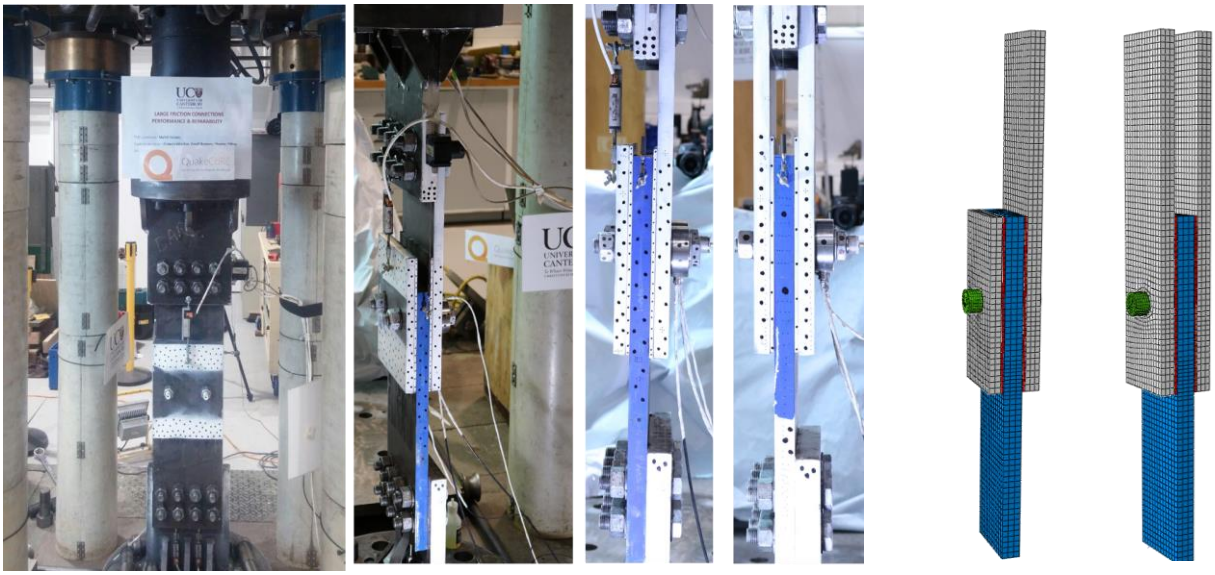

(a)Front view (b)Edge view (c)AFC (d)SFC (e) FEM meshes

Figure 2: AFC&SFC. Test setup using the DARTEC machine & numerical model meshing

The specimens were tested by Appling cyclic displacement protocol according to ACI report T1.1-01. Twenty four cycles were applied from ±1.25 mm to ±80 mm with eight different amplitudes to obtain 2625 mm cumulative travel. At the end of the first run sufficient time was allocated for the specimens to cool down and then the next runs were conducted. The minimum loading velocity was 1 mm/s up to ±40 mm displacements (cycle 1 to cycle 18). This increased to 3 mm/s for displacement of ±60 mm or greater (including cycle 19 to 24).

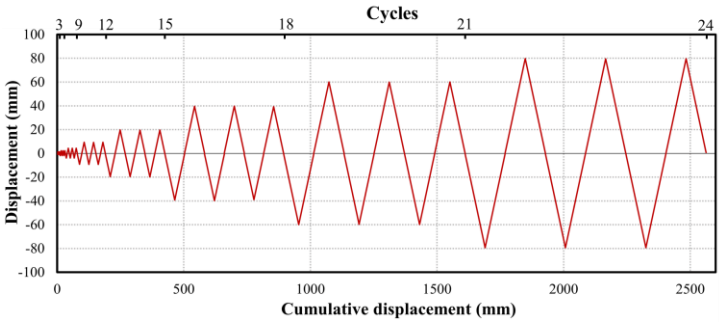

Figure 3: Loading protocol

3 FINITE ELEMENT MODEL

FE models were created for both the AFC and SFC tests. These were half width models with only one bolt and restrains were provided to model symmetry. Required material properties, contact interaction between plates, bolt shank, bolt head and nut (as surface-to-surface contact with different friction coefficients) and also material and geometry nonlinearity were defined and validated with the experimental tests and prior studies simulating AFC in bracing systems and base-column connections, Hatami et al. (2018). The static general method was implemented in this study using ABAQUS/Implicit. The meshed models are shown in Figure 1e. The mesh of the bolts and all plates were made by three-dimensional continuum 1st-order, reduced-integration hexahedral elements (C3D8R). Up to 20000 elements were used, and a mesh convergence procedure was used. Different contact areas between the surfaces, bolt head and nut with outer surfaces and the bolt shank with the plate holes defined using penalty and hard contact for tangential and normal friction models. The average friction coefficient which obtained from the experimental tests reported here.

4 RESULTS AND DISCUSSION

The SFC tests were started at a temperature of 18℃. In S#1 the temperature increased to 30℃ at ±40 mm displacement and gradually increased to 46℃ at the end of the 1st run. Before starting the 2nd run (S#2) the specimen was cooled down to about 26℃. The temperature increased continuously and reached 56℃ at the end of this run. The maximum observed temperature was at the end of S#5 was 90℃.In the AFC tests, the temperature rose 8℃ at the end of the 1st run, A#1 (from 21℃ to 29℃) and at the end of A#5, it reached 40℃.

There were no noise or vibration from the beginning to the end of the 1st run (S#1). Loose debris appeared in the form of black fine particles smaller than 1 mm. From the initial cycles of the 2nd run, loose debris fell off the specimen with various shapes and dimensions up to 1 mm. Although no vibration occurred in this run, and to the end of the last run (S#5), there was significant noise due to movement of loose particles over the sliding contact surfaces causing the formation of grooves, scratches and the polishing of the surfaces. In the AFC tests, significant noise and vibration occurred from a displacement ±20 mm in A#3. This continued in the following runs. The vibration caused 5 to 20 degrees nut rotation and increased the amount of bolt force loosening in the AFC. However, there was no nut rotation in the SFC. The number, length, width and/or depth of grooves increased after 5300 mm cumulative travel. This is after ±5 mm displacements in S#3. The larger removed particles were observed with different shapes such as flakes with the maximum dimension of 3-4 mm as shown in Figure 4a.

After all tests, the specimens were disassembled, and the surfaces inspected. In the SFC tests, damage on both sliding surfaces of the slotted plate was similar. It consisted of straight grooves alongside the slotted holes due to the formation of harder particles and surface ploughing and galling. Figures 4b and 4c show the damaged shim and the slotted plate at the end of S#5. Groove dimensions were in the range of 40 mm to 250 mm in length, 1 mm to 4 mm width and 1-3 mm in depth. In the AFC the significant damage occurred between the fixed and sliding plate. There was one groove 200 mm in length, 3 mm width and 2 mm depth. There was also three grooves less than 50 mm long with similar width and depth. Damage to the AFC shim and slotted plate are given in Figures 4e and 4f. The volume of removed material was almost 50% of that observed for the SFC.

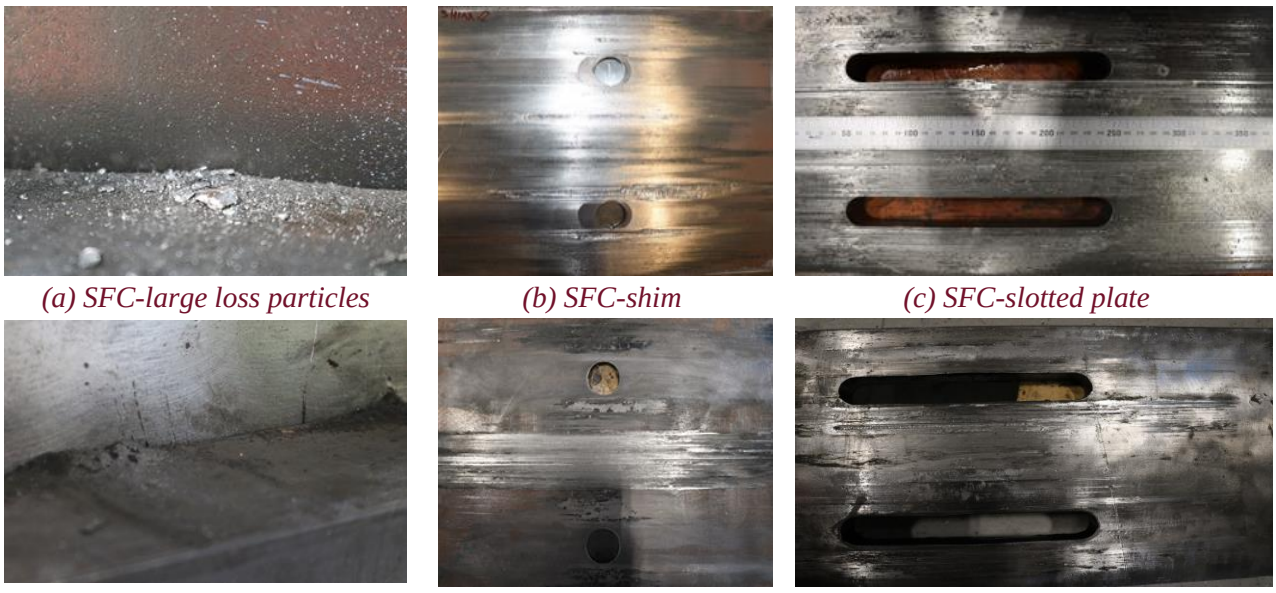

(a) SFC-large loss particles *(b) SFC-shim* *(c) SFC-slotted plate*

(d) AFC-fine particles *(e) AFC- shim* *(f) AFC-slotted plate*

Figure 4: Wear particles and the sliding surfaces after tests

Figure 5 shows the force-displacement response of the SFC and AFC subjected to the cyclic displacement regime. Tests specifications and a summary of findings are presented in Table 1.

The hysteresis loop shape for both AFC and SFCs was similar, but the strength ratio, defined as the ratio of SFC strength to AFC strength was as high as 3.28 in the 2nd run of both tests. In the AFC initial sliding occurs on one side of the slotted plate, where there is no relative movement between the slotted plate and the cap plate. The second sliding happens between the slotted plate and the cap palate where the AFC reach the maximum sliding force. However, in SFC the slotted plate moves between the two fixed plates, so two sliding surfaces are activated at the same time.

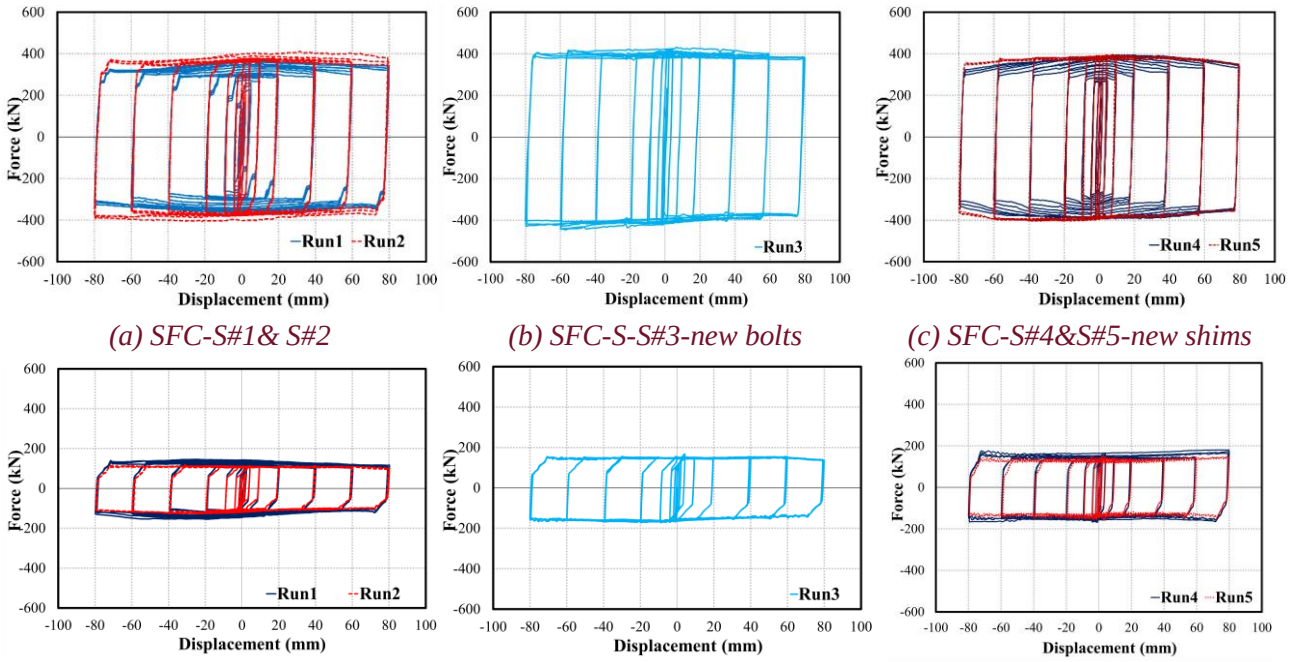

(a) SFC-S#1& S#2 *(b) SFC-S-S#3-new bolts* *(c) SFC-S#4&S#5-new shims*

(d) AFC-A#1& A#2 *(e) AFC-A#3-new bolts* *(f) AFC-A#4& A#5-new shims*

Figure 5: Experimental test results- Hysteresis Loops

In S#1 the initial sliding force on one side of the slotted plate was 160 kN as shown in Figure 5a. The strength increased to 290 kN for sliding on both sides after nine cycles (±5 mm) as shown in Table 1 by $V_{initial}$. The strength increased gradually within all cycles, however, after initial cycles the average tension and compression strength stabilised to 340 kN as. An effective friction coefficient of 340 kN/(2× 2 ×210 kN)=0.405 was computed for this stable strength, where 210 is the bolt proof load, and there are two bolts and two sliding surfaces. The strength reached a maximum of 371 kN after 2560 mm cumulative travel of the slotted plate (displacement ±80 mm) as shown in Figure 5a. After the first run, the specimen was cooled down and the test repeated without bolt retightening. It may be seen that the 2nd run (S#2) displayed more stable behaviour with the initial stable strength of 345 kN at ±5 mm which almost plateaued to the strength of 365 kN to the end of this run. The minimum sliding force on one side of the slotted plate was 60% larger than what was in the first run. Also, the maximum strength was 410 kN in this run (10% larger than the 1st run). The 3rd run (S#3) was conducted with the new bolts and displayed a more stable hysteresis loop than other runs with the highest strength of 446 kN at the peak point, as given in Figure 5c. The initial strength at the first cycle (±1.25 mm) on only one side of the slotted plate was 235 kN which immediately after four cycles increased to 400 kN at displacement ±2.5 mm, and remained almost constant to the end of the test.

Degradation increased in this run (S#3) compared to S#1 and S#2. The degradation was defined as the maximum strength divided by the final cycle strength in that run at zero displacement. It was 0.3% in S#1, increased to 12% in S#2 and reached a maximum of 15% in S#3 between all five SFC runs. Figure 5c shows the hysteretic behaviour of SFC with the replaced shims and bolt in S#4 which repeated after 2625 mm cumulative travel in S#5. Degradation in the 4th run was almost zero because the maximum strength occurred at the end of the run at the zero displacement. The hysteresis loop shape was similar to that of the first run where significant strength increase was observed during the sliding. This behaviour was expected as a result of new sliding surfaces between the new shims and worn surfaces on the slotted plate. The maximum strength reached 392 kN which was 6% larger than the 1st run at the beginning of the test and 12% lesser than the 3rd run with the new bolts and the sliding surfaces which had been used and worn in the 1st and 2nd runs. S#5 as the last run on the specimen with the slotted plate which had 10500 mm cumulative travel and the shims were replaced after the S#3. This test is a repeat of S#4. It displayed more stable behaviour compared to the other four runs. The initial sliding force was 300 kN which gained to 380 kN rapidly after only four cycles (±2.5 mm) as the initial stable strength ($V_{initial}$) and reached the stable strength of 385 kN after 35 mm cumulative travel (±5 mm). Degradation was 10% in this run which was higher than the 4th run and lesser than the 2nd run.

Figures 5d to 5f show the AFC hysteretic behaviour for five different runs. The overall behaviour was stable with the maximum strength ranging from 125 kN to 180 kN and almost rectangular shape. In A#1 as the 1st run, the initial sliding force on one side of the slotted plate was 86 kN which increased to 102 kN after 6 cycles (displacement ±2.5 mm) and reached 123 kN after 9 cycles (±5 mm) as $V_{initial}$ in Table1 which was 5% less than the stable strength of 130 kN through the sliding and 25% less than the maximum strength of 154 kN which occurred after 1950 mm cumulative travel in the last cycles (displacement ±80 mm). The strength at zero displacement at the end of this run reduced to 123 kN which means 20% degradation. The strength variation is defined as the difference between the peak strength, the initial strength and the stable strength (in Table 1) reduced in the 2nd run (A#2) compared to the 1st run. In the 2nd run where testing was repeated, and the maximum strength to the stable strength ratio of 1.09 was observed and the degradation reduced to 8.0% (28% degradation after 5250 mm cumulative travel).

The bolts were replaced, and the run A#3 was conducted. As shown in Figure 5e, the hysteresis loop is more stable compared to the 1st and 2nd runs. The initial strength was 130 kN which increased to 154 kN at the initial stable strength and increased to 164 kN at the peak point. The strength degradation decreased to 6.0% as the minimum magnitude of all AFC runs. The force-displacement response of the 4th and 5th runs (A#4 and A#5) with the new shims and bolts are shown in Figure 5f. The strength was stabilized after three initial cycles and reached 150 kN and remained almost consistent until the cycle 18 (displacement ±60 mm).in the last three cycles (displacement ±80 mm) as a result of damaged sliding surfaces and induced vibration, and the strength increased to 180 kN with fluctuation and instability. The maximum strength of 180 kN was the largest strength compared to other runs. The strength degradation was similar to the 1st run of 20% which reduced to 16% at the end of A#5 as the repeated test. The strength reached the stable value of 135 kN after six cycles (displacement ±2.5 mm) and remained almost constant to the end of the test.

In this table; $V_{initial}$ is the force at ±5 mm displacement (cycle 9, 88 mm cumulative travel), as the initial stable friction force where the slotted plate moved between two surfaces. V_{peak} is the maximum force in the test, and V_{stable} is the steady state of sliding force (average tension/compression) after the initial state, where the initial stable sliding force is reached the end of the run. Bolt force ratio is defined as the ratio of the bolt force at the end of each run divided to the initial bolt force before the beginning of the test. $\boldsymbol{\mu_{effective}}$ is the sliding force (V_{stable}) divided by the total proof load **(**2×210 kN) and the number of friction surfaces (2). This is 2 ×2×210=840 kN.

Table 1: Summary of results

	Test	Specification	$V_{initial}$ (kN)	V_{peak} (kN)	V_{stable} (kN)	$\frac{V_{peak}}{V_{initial}}$	$\frac{V_{peak}}{V_{stable}}$	$\frac{V_{initial}}{V_{stable}}$	Bolt force ratio (%)	$\mu_{effective}$
SFC	S#1	1st run	290	371	340	1.28	1.09	0.85	7%	0.40
	S#2	Repeat	345	404	365	1.17	1.11	0.95	9%	0.43
	S#3	New bolts	385	446	400	1.16	1.12	0.96	10%	0.48
	S#4	New Shims	278	392	335	1.41	1.17	0.83	12%	0.40
	S#5	Repeated	380	402	385	1.06	1.04	0.99	15%	0.46
AFC	A#1	1st run	123	154	130	1.25	1.18	0.95	33%	0.15
	A#2	Repeat	105	125	115	1.19	1.09	0.91	45%	0.14
	A#3	New bolts	154	160	148	1.04	1.08	1.04	30%	0.18
	A#4	New Shims	148	180	150	1.22	1.20	0.99	20%	0.18
	A#5	Repeated	130	155	135	1.19	1.15	0.96	27%	0.16

Figure 6 shows the bolt force changes during the sliding and a comparison of friction coefficient. The bolts were initially tightened to 210 kN as the bolt proof load of M24 bolts. Figure 6a shows in SFC first two runs the bolt tension force during the sliding remained almost constant in the range of 191 kN to 210 kN. The bolt force reduced to 93% at the end of the 1st run and to 91% of the initial value at the end of the 2nd run as shown in Figure 5a. The loss of bolt force was almost the same with 2.0% to 3.0% increase for the next three runs. The maximum of bolt force reduction was in S#5 with the reduction of 15% of the initial force. However, the bolt behaviour was different in the AFC as shown in Figure 5d. The test started a few minutes after tightening, which caused a bolt force reduction of 10 kN before starting the test. This 10/210=4.8% decrease in axial tension force before sliding maybe due to self-loosening or creep. In the 1st run, the initial force rapidly reduced to 186 kN after three cycles (cumulative 15 mm) and then to 170 kN after ten cycles (cumulative travel 175 mm, displacement ±10 mm). The bolt force reduced gradually and reached 153 kN (77% of the tension force at the beginning of the test) after 1320 mm cumulative travel (displacement ±60 mm) and continued to the end of the test. The bolt force at the end of the 2nd run (after 5250 mm cumulative travel) reduced to 110 kN which means 74% of the initial force at the beginning of the 2nd run and 55% of the initial bolt force at the beginning of the 1st (A#1). Loss of the preloading force reduced to 70% of the initial force at the end of the 3rd run with the replaced bolts. The minimum reduction in the bolt force was occurred in the 4th run (with the new bolts and shims) which was of 20% of the initial force. A#5 exhibited the minimum bolt force reduction compared to other runs. The reduction was 7.0% within this run.

The instantaneous coefficient of friction was calculated as the sliding force divided by the instantaneous bolt tension force during the sliding tests as shown in Figure 6b and 6c for SFC and Figure 6e and 6f for AFC. In S#1 as the 1st run friction coefficient on one side of the slotted plate was 0.2 at initial 3 cycles (displacement ±1.25 mm) and 0.4 after 148 mm cumulative travel (displacement ±10 mm) and remained almost constant to the end of the test, however, the maximum friction coefficient reached 0.47 after 2340 mm cumulative travel (displacement -80 mm) in compression. As the result of only 10% variation in the bolt force in SFC, there were negligible differences between the instantaneous friction coefficient and the effective friction coefficient in Table 1. In the 2nd run as discussed before the worn sliding surfaces represented more stable behaviour. The friction coefficient reached almost 0.46 after seven cycles (displacement ±5 mm) and remained almost constant to the end of the test. The friction coefficient in the SFC with the new shims and bolts (S#4) was 0.4 after 320 mm cumulative travel and reached a peak of 0.53 at the end of the test. However, the average friction coefficient was 0.46. For the last run (S#5) the plates which had been used and degraded within the 10500 mm cumulative displacement the friction coefficient was almost 0.5 from the initial cycles to the end of the test.

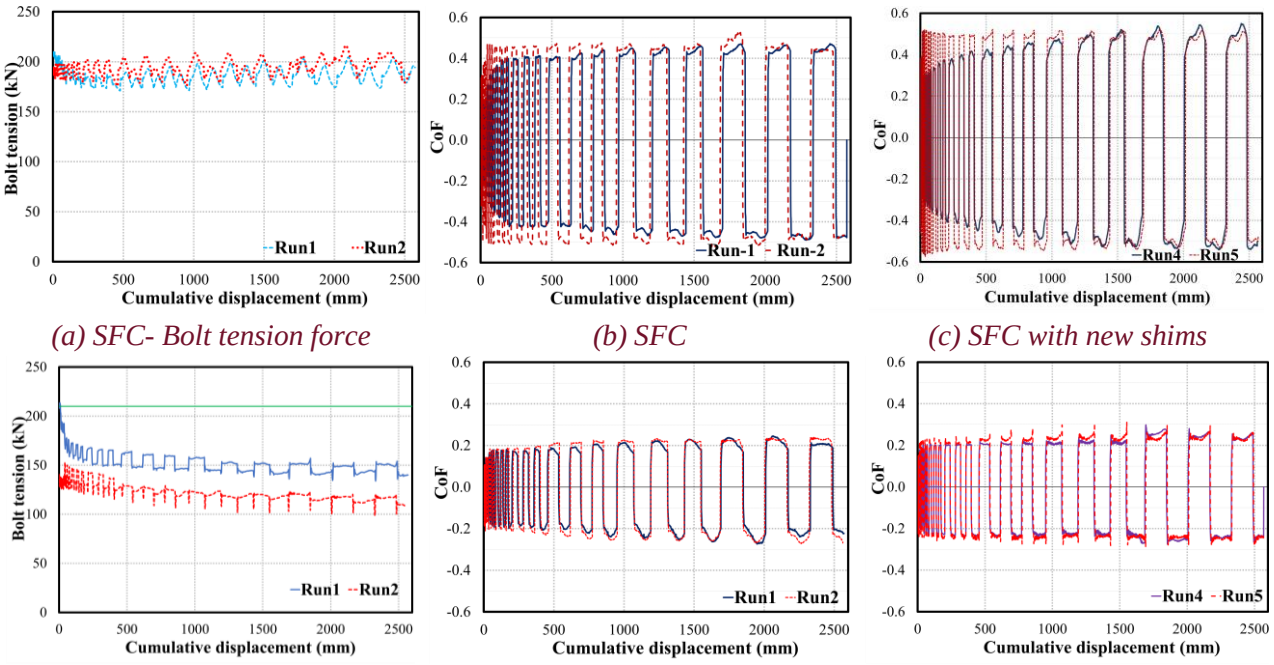

(a) SFC- Bolt tension force *(b) SFC* *(c) SFC with new shims*

(d) AFC- Bolt tension force *(e) AFC* *(f) AFC with new shims*

*Figure 6: The bolt force during sliding and instantaneous **C**oefficient **o**f **F**riction*

Figure 6e shows the instantaneous friction coefficient in AFC 1st run (A#1) at initial cycles was 0.16 which increased to 0.19 after 65 mm cumulative travel (displacement ±5 mm) and reached the peak of 0.27 at 1961 mm cumulative travel(displacement ±80 mm). The stable friction coefficient was 0.2 for this run. The 2nd run showed a similar trend to the 1st run with the maximum instantaneous friction coefficient of 0.28 after 2270 mm cumulative displacement. The effective coefficient of friction for these two runs was 0.15 and 0.14 respectively. The instantaneous friction coefficient for AFC with new shims and bolts is shown in Figure 6f. It was 0.21 after six cycles and increased to 0.25 rapidly as the stable friction coefficient for the 4th and 5th runs. However, the maximum of 0.3 was observed after 1072 mm cumulative travel. The effective friction coefficient ($\mu_{effective}$) was 0.18 and 0.16 for the last two runs as shown in Table 1.

Adhesive wear at first cycles and two-body and three-body abrasive wear for larger cycles were the dominant wear mechanism. The strength hardening/growing was due to (i) increasing the real contact area between the sliding surfaces at the beginning of sliding which increase the adhesion, (ii) ploughing and wedge formation on sliding surfaces (the slotted plate and then shims with harder materials) as a result of trapped wear particles between the slotted plate and shims and microscale and macroscale interlocking between surfaces (iii) temperature rise causing the plates move out, and push more on the bolts and (iv) strain hardening of the slotted plate in the damaged area. Fallen out particles also result in grip length reduction and reduce the initial bolt elongation. In the AFC the smooth sliding of the slotted plate within the 2nd and 3rd runs confirmed the stable sliding condition with the higher friction coefficient because of the formation of smooth surfaces after the first run due to polishing surfaces. In addition, no large picked-up particles were originating from the breaking of the asperities at slotted plate surfaces in contact with the shims. The volume of loose debris (as small black particles) was approximately 50% of that in the first run and significantly less than the SFC tests. All the plates were easily disassembled without any cold welding as expected because of the low loading rate.

Two different models were developed for AFC and SFC. The 2nd run of each test was selected, and the FEM calibrated with the stable instantaneous friction coefficient. The FEM, like the tests, has different sliding force values in compression and tension. However, it does not show the strength increase or decrease in the actual tests because of the removal of particles.

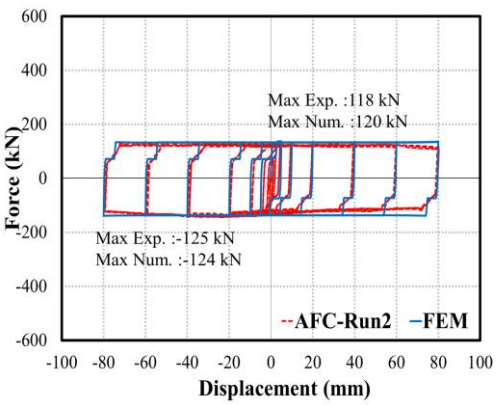

(a) AFC hysteresis loop - FEM

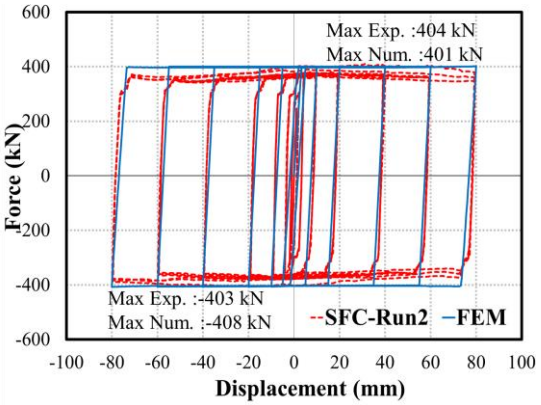

(b) SFC hysteresis loop - FEM

Figure 7: FEM validation with experimental tests

In the 2nd run, the overall behaviour was more stable with a lesser strength degradation. Figure 7a and 7b show the FEM represented the behaviour of experimental tests with the minimum variation. In AFC the maximum strength in tension was 118 kN and 125 kN in compression which was similar in the FEM with less than 2.0% difference. In FEM the sliding force on one side of the slotted plate was 66 kN. The strength increased to 124 kN for sliding on both sides. From the displacement +40 mm to the end of the test the maximum strength in compression was lesser than that in FEM (84%). Figure 7b shows in the SFC model the maximum strength was 408 kN and 404 kN in compression and tension respectively. In the FEM the maximum strength in tension was 3.0 kN lesser and 5 kN larger than that in the experimental test.

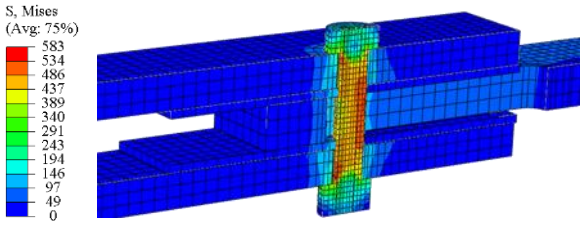

(a) SFC- tension (Disp. +80 mm)

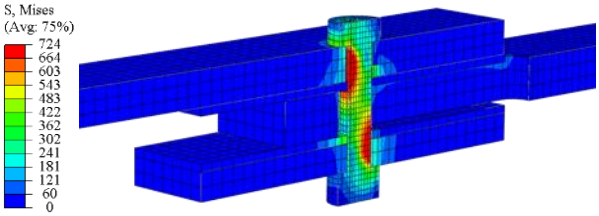

(b) AFC- tension (Disp. +80 mm)

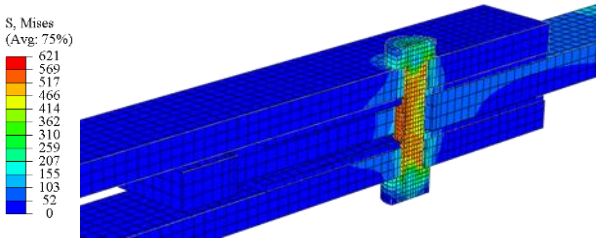

(c) SFC- compression (Disp. -80 mm)

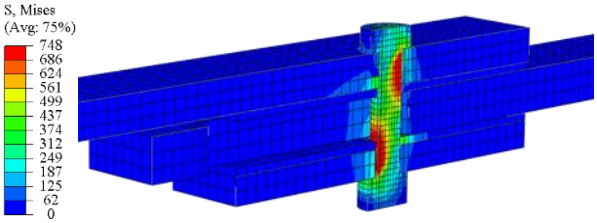

(d) AFC- compression (Disp. -80 mm)

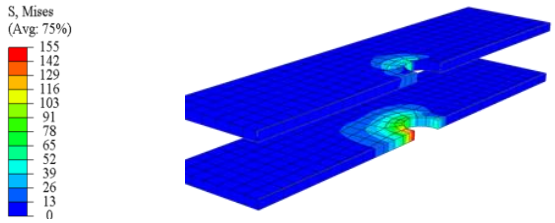

(e) SFC- Shims (Disp. +80 mm)

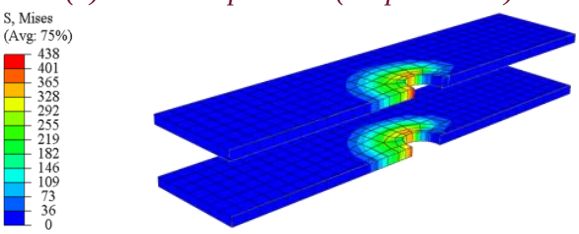

(f) AFC- Shims (Disp. +80 mm)

Figure 8: Von Misses stress distribution in the AFC & SFC components.

Figure 8 shows the stress distribution in the AFC and SFC at a displacement of ±80 mm. In the SFC the maximum Von Misses stress before sliding was 530 MPa. When the slotted plate was pulled, the maximum stress reached 583 MPa. The bolt was straight in contact with the fixed plates at top and bottom which act as a support. The maximum stress was 283 MPa at the fixed plate holes indicating no yield. The bolt was loaded by the two shims 44 mm apart. The stress concentration occurred at this length. The maximum stress in the bolt reached 620 MPa in compression with same distribution on the reverse side of the bolt shank. By tack welding the shims to the fixed plates, the shims do not move. Therefore they do not bear against the bolts. SFC bolt stresses reduced 3.0% in compression. However, the bolt bending stresses due to shims movement were almost eliminated, and there was no stress concentration. This is a way to improve SFC performance further. In AFC the maximum stress of the bolt shank after tightening to the proof load was 520 MPa which increased to 724 MPa and 748 MPa in tension and compression respectively as shown in Figures 8b and 8d. The maximum stresses on the bolts occurred between the fixed and cap plates. The bolt lever arm (i.e. the distance between the points with the maximum stress) is the length that the shear sliding force imposes to the bolt. The maximum stress in the steel shim plate reached 438 MPa and 155 MPa in the SFC and AFC respectively which shows no plastic deformation occurred at this region as shown in Figures 8e and 8f.

5 CONCLUSION

This paper described the experimental and numerical behaviour of the AFC, and the SFC with two M24 Grade 8.8 high strength structural bolts and fully wire brushed surfaces to a cyclic displacement regime. It was shown that:

1. There were no noise or vibration in SFC, however, in AFC after the 2nd run significant noise and vibration were observed. SFC damage, regarding a number of grooves, shape and size of loose debris was significantly larger than for the AFC in this case. The maximum temperature in AFC increased by 19℃ while in SFC rose 72℃. This temperature increase is roughly proportional to the amount of hysteretic energy dissipated.
2. The hysteresis loop shape was almost rectangular and stable within during the sliding even after 13125 mm cumulative travel of the slotted plate. Although the initial clamping force in the bolts and sliding surfaces were similar, the shear sliding force in SFC was 2.20 to 3.30 times bigger than the AFC.
3. The maximum bolt tension loss was 15% and 45% in the SFC and AFC respectively. The effective coefficient of friction was in the range of 0.40 to 0.48 in the SFC. The instantaneous friction coefficient was almost similar due to the stable bolt force during the sliding with the maximum value of 0.53 at the peak points. The effective coefficient of friction in AFC was between 0.14 and 0.18, where the maximum instantaneous friction coefficient was 0.3.
4. In repeated runs, without changing the specimen, the strength of the AFC decreased by up to 12% while that for the SFC increased by up to 9.0%. The maximum strength degradation was 15% and 20% for the SFC and AFC respectively. Both the AFC and SFC were reparable with new bolts and/or new shims after 13125 mm cumulative travel. The SFC is much more effective in providing strength and dissipating energy.

6 ACKNOWLEDGEMENTS

This research was supported by the University of Canterbury, John Jones Steel, Steel and Tube, Fletcher Steel and Vulcan Steel. Also, this project was (partially) supported by QuakeCoRE, a New Zealand Tertiary Education Commission-funded Centre. This is QuakeCoRE publication number 420.

7 REFERENCES

Bisalloy Steels. 2015. *Bisplate technical guide*. http://www.bisalloy.com.au/contents/technical-information-for-BISPLATE®-product

Chanchi, J., MacRae, G.A., Chase, J.G., Rodgers, G.W., Mora, A. & Clifton, G.C. 2012. *Design considerations for braced frames with asymmetrical friction connections-AFC*.

Clifton, G.C. 2005. *Semi-rigid joints for moment-resisting steel framed seismic-resisting systems*, ResearchSpace@ Auckland.

DAKOTA. 2019. http://dakotaultrasonics.com/product/bolting-products-2/bolting-products/.

FitzGerald, T.F., Anagnos, T., Goodson, M. & Zsutty, T. 1989. Slotted bolted connections in aseismic design for concentrically braced connections, *Earthquake Spectra*, Vol 5 383-91.

Golondrino, J., Chanchi, G.M., Chase, J. Rodgers, J. & Clifton, C. 2016. *Effects of the bolt grip length on the behaviour of Asymmetrical Friction Connections (AFC)*.

Grigorian, C.E. & Popov, E.P. 1994. *Energy Dissipation with Slotted Bolted Connections* (Earthquake Engineering Research Center, University of California).

Hatami, M., MacRae, G., Rodgers, G.W. & Clifton, G.C. 2018. Numerical Study of Asymmetric Friction Connections (AFC) with Large Grip Length Bolts, *Key Engineering Materials*, 600-08. Trans Tech Publ.

HBM. 2019. https://www.hbm.com/en/.

HYTORC. 2019. https://hytorc.com/electric-tools.

LCM SYSTEMS. 2019. http://www.lcmsystems.com/WAS_Force_Washer_Through_Hole_Load_Cell.

MacRae, G.A., Clifton, G.C., Mackinven, H., Mago, N., Butterworth, J. & Pampanin, S. 2010. The sliding hinge joint moment connection, *Bulletin of the New Zealand Society for Earthquake Engineering*, Vol 43 202.

Mitutoyo. 2019. https://ecatalog.mitutoyo.com/Surftest-SJ-210-Series-178-Portable-Surface-Roughness-Tester-C1794.aspx.

MOLYBOND. 2019. https://www.itwpf.com.au/molybond-lubricants/.

Standards New Zealand. 2009. *NZS 3404: Steel structures standard Part 1: Materials, fabrication, and construction*. Wellington, New Zealand: Standards New Zealand.

Pall, A.S. & Marsh, C. 1982. Response of friction damped braced frames, *Journal of Structural Engineering*, Vol 108 1313-23.

Standards New Zealand. 2016. *AS/NZS 1252:2016 High-Strength Steel Bolts with Associated Nuts and Washers for Structural Engineering*, In. Wellington-New Zealand.

Tremblay, R. 1993. *Seismic behavior and design of friction concentrically braced frames for steel buildings*, University of British Columbia.

Yang, T-S. & Popov, E.P. 1995. *Experimental and analytical studies of steel connections and energy dissipators* (Earthquake Engineering Research Center, University of California).